LBNL Eng. Note: SU-1010-4838

Documentation for USER102: a 2D User-Defined Electromagnetic Element in ANSYS

Lucas Brouwer

ATAP Division, Lawrence Berkeley National Laboratory

Documentation is given for a user defined 2D electromagnetic element in ANSYS. This element is formulated similar to the standard distribution PLANE53, but includes both quench behavior and interfilament coupling losses in the conductor region. This element can be coupled to USER101 to include transient thermal behavior.

Contents

1 Element Form and DOF

Similar to PLANE53, the higher order element USER102 has four midside and four corner nodes with labeling as seen in Figure 1. This element can be used with two different sets of degrees of freedom (DOF) selected using element key options. The first option uses a single DOF (axial vector potential A_z) at all nodes which is compatible with applied current density loading. A second option allows the element to be coupled to an external circuit as a stranded coil. This is accomplished by adding a voltage drop $e(t)$ and current per turn $i(t)$. The DOF are interpolated throughout the element using the shape functions given in Equation 1. Integration of functions over the element, as needed for the generation of element matrices, is performed numerically using Gaussian quadrature with four integration points. The location of the four sampling points and their corresponding weights can be found in the ANSYS theory manual or introductory finite element textbooks [1, 2].

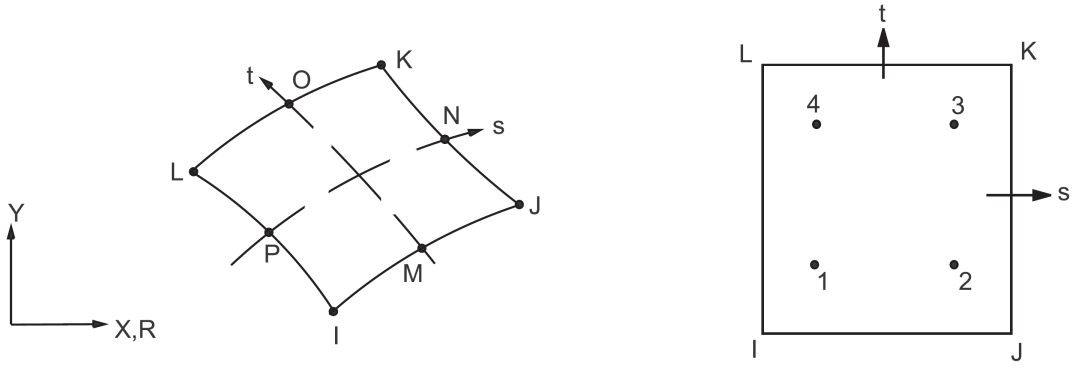

Figure 1: The ordering of the 8-node element geometry is shown on the left, and again for the four Gaussian quadrature points on the right (Figs from [1], Pg. 640 and Pg. 482).

$$
\begin{aligned}
u = &+ \frac{1}{4}u_I(1-s)(1-t)(-s-t-1) \\
&+ \frac{1}{4}u_J(1+s)(1-t)(+s-t-1) \\
&+ \frac{1}{4}u_K(1+s)(1+t)(+s+t-1) \\
&+ \frac{1}{4}u_L(1-s)(1+t)(-s+t-1) \\
&+ \frac{1}{2}u_M(1-s^2)(1-t) \\
&+ \frac{1}{2}u_N(1+s)(1-t^2) \\
&+ \frac{1}{2}u_O(1-s^2)(1+t) \\
&+ \frac{1}{2}u_P(1-s)(1-t^2)
\end{aligned}
\tag{1}
$$

2 Keyopts and Real Constants

Similar to standard distribution elements, USER102 has several element key options used to define element properties. These are outlined in Table 1. Key option 1 defines the DOF for the element with options for stand alone use (with applied current density loading) or external circuit coupling. Key option 2 specifies whether the element will be coupled to the thermal user element USER101 using the Multi-field Solver. This requires mapping of the element numbers between electromagnetic and thermal domains and also enables binary file writing for passing of non-standard Multi-field Solver variables. More detials and additional set up steps for coupling between the user elements are outlined in Section 6. Key options 3 and 5 are used to select the critical current density parametrization and copper resistivity fit. Key options 7 and 8 are used as flags to define quench and interfilament coupling current behavior.

Table 1: USER102 Key Options

Selection	Keyopt	Value	
DOF	(1)	0	AZ (Je driven conductor)
		1	AZ,VOLT (hold for future development)
		2	AZ,CURR,EMF (circuit coupled conductor)
Field transfer with thermal [1]	(2)	0	no
		1	yes
Jc fit function [2]	(3)	0	see Equation 2
		1	hold for future development
		2	userJc.f (hold for future development)
Cu - rho fit (T,B) [3]	(5)	0	ANSYS table (T only)
		1	NIST (T,B,RRR)
		2	CUDI (T,B,RRR)
		3	MATPRO (T,B,RRR)
		4	userCu.f (hold for future development)
Quench flag [4]	(7)	0	check for quench (with current sharing)
		1	force superconducting
		2	force fully quenched
		3	check for quench (no current sharing)
IFCC flag [5]	(8)	0	allow IFCC, tau calculated
		1	no IFCC
		2	allow IFCC, fixed tau from real const. 11

[1] using the Multi-field Solver as described in Section 6
[2] form is $J_c = J_{c0}(1-t^p)^{\alpha-1}(1-t^2)^{\alpha}h^{-.5}(1-h)^2$ with real const. 13-17 (see Section 3)
[3] cu RRR set by real const. 8, see [3] for more details
[4] see Section 3 for current sharing behavior, option 3 is an abrupt transition at $J_{cw} = J_c$
[5] tau can be scaled with real const. 12

Real constants are used to specify the geometry and properties of the modeled coil regions. The total coil region area is set by S_c, and can contain both conductor and some matrix material (assumed to be epoxy for the thermal element). The fraction of this total area which is occupied by conductor is set using f_{cond}, and the fraction of this conductor area which is made up of superconducting material is set using f_{sc}. The total number of conductor turns in the coil region is set by N_c, and the residual resistivity ratio of the stabilizing copper is set by RRR. Other parameters are given in Table 2, along with a specification of which real constants are needed based on the value of key option 1.

Table 2: USER102 Real Constants

Real Const.	Variable		Req. Keyopt
(1)	S_c	area of modeled coil region	(1)=2
(2)	N_c	number of turns in coil region	(1)=2
(3)	f_{cond}	fraction of conductor in coil region	(1)=0,2
(4)	f_{sc}	fraction of superconductor in conductor region	(1)=0,2
(5)	$dirz$	current direction (+1=+z, -1=-z)	(1)=2
(6)	L_c	effective length for coil resistance (physical)	(1)=2
(7)	L_i	effective length for coil inductance (magnetic)	(1)=2
(8)	RRR	RRR of the copper stabilizer	(1)=0,2
(9)	L_p	filament twist pitch	(1)=0,2
(10)	f_{eff}	IFCC scaling parameter for stabilizer resistivity	(1)=0,2
(11)	τ	fixed IFCC time const. for keyopt(8)=2	(1)=0,2
(12)	τ-mult	scale factor for τ	(1)=0,2
(13)	J_{c0}	Nb_3Sn Jc fit parameter (in Equation 2)	(1)=0,2
(14)	T_{c0}	Nb_3Sn Jc fit parameter (in Equation 2)	(1)=0,2
(15)	B_{c0}	Nb_3Sn Jc fit parameter (in Equation 2)	(1)=0,2
(16)	α	Nb_3Sn Jc fit parameter (in Equation 2)	(1)=0,2
(17)	p	Nb_3Sn Jc fit parameter (in Equation 2)	(1)=0,2
(18)	IFCU-mult	scale factor for current sharing fraction IFCU	(1)=0,2

3 Quench Behavior

3.1 Critical Current Fit

At this time, the form of the critical current fit is set up for Nb_3Sn. If a different superconducting material or parametrization is desired, the quench module file quench.f can be modified. The default parametrization fit function is given by

$$J_c = J_{c0}(1-t^p)^{\alpha-1}(1-t^2)^{\alpha}h^{-.5}(1-h)^2 \tag{2}$$

where

$$t = \frac{T}{T_{c0}}, \tag{3}$$

$$B_c = B_{c0}(1-t^p), \tag{4}$$

$$h = \frac{B}{B_c}, \tag{5}$$

with fit parameters J_{c0}, T_{c0}, B_{c0}, α, and p input as real constants as described in Table 2.

3.2 Current Sharing

The use of a stranded approach, with uniform current density for all elements in a modeled coil region, is motivated by modeling of multifilamentary conductors typical of Nb-Ti and Nb_3Sn magnets. While this does not allow for the solution of the distribution of current within the mix of stabilizing material and superconductor, the effect of current sharing and quench on the resistive joule heating is included on the element level using three distinct regimes. These are summarized in Table 3, where I_{fcu} represents the fraction of current in the stabilizer.

Table 3: Quench States

qflag value	Regime	Fraction of Current in Stabilizer
-1	Fully Superconducting	$I_{fcu} = 0$
0	Current Sharing	$0 < I_{fcu} < 1$
1	Fully Quenched	$I_{fcu} = 1$

When operating below the critical surface, all current is assumed to be flowing in the superconductor such that the element is fully superconducting and has no ohmic loss. If the combination of field, current density, and temperature rise to a level where the operating point is above the critical surface, a fraction of the current is assumed to move into the stabilizer to maintain a current density in the superconductor which is below the critical surface. This current sharing continues up to the point at which the temperature and field is such that no current density can flow in the superconductor. The element is then considered fully quenched, with all current flowing in the stabilizer and the resistance loss maximized.

Accurate assumptions for the variation of I_{fcu} during current sharing is dependent on the superconducting material and the significance of this quench state to magnet behavior being simulated. An exhaustive review of this topic is found in Chapter 18 of [4]. A common assumption for Nb_3Sn and Nb-Ti conductor is a linear variation of I_{fcu} from T_{cs} to T_{cB} [5].

At each element matrix generation call, the following steps are taken to determine the element quench state (qflag) and fraction of current assumed to be in the stabilizer for this element (I_{fcu}). The current density in the superconducting fraction of the conductor region J_{cw} is calculated as

$$J_{cw} = \frac{J_e}{f_{cond} f_{sc}}, \tag{6}$$

for keyopt(1)=0 with applied current density J_e, or

$$J_{cw} = \frac{i(t) N_c}{S_c f_{cond} f_{sc}}, \tag{7}$$

for keyopt(1)=2 with coupling as a stranded conductor to an external circuit. The critical current density J_c is then calculated using Equation 2 and the average element magnetic field and temperature. The current sharing parameter is then set using

$$I_{fcu} = \begin{cases} 0 & J_{cw} \leq J_c \\ 1 - \frac{J_c}{J_{cw}} & J_{cw} > J_c \ \ \& \ \ T < T_{cB0} \\ 1 & T \geq T_{cB0} \end{cases} \tag{8}$$

where T_{cB0} is the temperature at which the superconductor can carry zero current at the average element field $T_{cB0} = T_{cs}(0, B)$. With the parametrization in Equation 2, this is given by

$$T_{cB0} = T_{c0} \left(1 - \frac{B}{B_{c0}} \right)^{\frac{1}{p}}. \tag{9}$$

4 Interfilament Coupling Currents

Interfilament coupling currents (IFCC) are an important loss mechanism for superconducting magnets. Their relatively short time constant (tens of milliseconds or less) and localized heat deposition within the strand make them an effective mechanism for magnet quench back. As shown in Fig. 2, these induced currents flow along the superconducting filaments which are twisted along the length of the strand and then across the strand matrix.

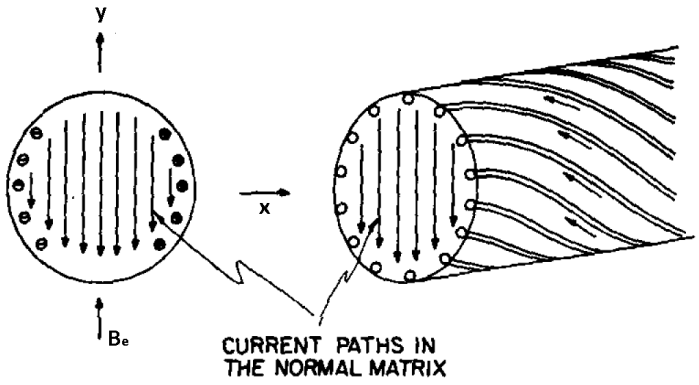

Figure 2: The path of interfilament coupling currents induced by a changing vertical field is shown (Fig. from [6]). The current flows along the twisted filaments and then across the strand matrix. This results in strand magnetization as well as resistive losses in the matrix material.

For a uniform field change within the strand, the induced axial current is typically approximated using a cosine theta (dipole producing) current density [6, 7]

$$g_z(\theta) = \dot{B}_i \left(\frac{L}{2\pi}\right)^2 \frac{cos(\theta)}{\rho_{et}}, \tag{10}$$

where $\dot{B}_i$ is the vertical field change within the strand, L is the filament twist pitch, and ρ_{et} is the effective resistivity of the strand matrix. To include contact resistance between matrix and filaments, the effective resistivity is defined as $\rho_{et} = f_{eff} rsvx$ where $rsvx$ is the stabilizer resistivity and f_{eff} is input as real constant 10. If B_e is an applied, uniform external vertical field, the field within the strand is depressed by the induced IFCC currents as

$$B_i = B_e - \frac{1}{2}\mu_0 g_z(\theta = 0) \tag{11}$$

$$B_i = B_e - \tau \dot{B}_i, \tag{12}$$

where the natural time constant for the induced current is clearly

$$\tau = \frac{\mu_0}{2\rho_{et}} \left(\frac{L}{2\pi}\right)^2. \tag{13}$$

The strand magnetization is then given by

$$M_e = -\frac{4}{\mu_0 \pi} \int_0^{\pi/2} g_z(\theta) cos(\theta) d\theta \tag{14}$$

$$M_e = -\frac{2\tau}{\mu_0} \dot{B}_i. \tag{15}$$

For those reviewing this approach in Wilson's textbook [7], it is helpful to note there is a missing μ_0 in Equation 8.51 (to match Equation 15). Section 8 shows how this equivalent magnetization approach to modeling IFCC can be added to the vector potential formulation, leading to the addition of a curl-curl term in the damping matrix of the FEM. These induced currents deposit energy as heat within the strand matrix with a power per unit volume of

$$P_e = \vec{M}_e \cdot \frac{\partial \vec{B}}{\partial t}, \tag{16}$$

which in many cases leads to IFCC losses being a highly effective quench back mechanism.

5 Joule Heating

The two sources of element heating are resistive loss due to quench and interfilament coupling currents. These losses are homogenized to account for fill factors of conductor and superconductor within the modeled coil region. The parameter f_{cond} is used to define the fraction of the total coil area which is conductor, and f_{sc} to define the fraction of superconductor within this conductor area. Quench induced loss is assumed to occur only within the stabilizer of the conductor, with the magnitude dependent on the quench state (see Table 3) and the resistivity of the stabilizing material. The power per unit volume of modeled conductor is then given by

$$JH_{res} = rsvx \ \frac{(I_{fcu}J_e)^2}{f_{cond}(1-f_{sc})} \tag{17}$$

for quench based loss, and

$$JH_{tau} = 2\tau \frac{f_{cond}}{\mu_0} \left| \frac{dB}{dt} \right|^2 \tag{18}$$

for losses resulting from interfilament coupling currents (see Equation 16). For a given quench state, the temperature and field dependence of these losses is driven by the variation of the stabilizer's resistivity. For Nb-Ti and Nb_3Sn this stabilizer is typically a high RRR copper, resulting in $rsvx$ (and then also τ) showing strong temperature dependence and magnetoresistive behavior.

6 Use with the Multi-field Solver

The Multi-field Solver is a documented feature of ANSYS which allows for solving of sequentially coupled problems with independent meshes [8]. A unique, meshed region is generated for each physics field and load coupling interfaces for which loads will be passed between them are specified. Each region is solved independently with its own time stepping and solution options. The solver transfers the loads across the defined interfaces (even with dissimilar meshes), and iterates between each physics field in sequence until the transfer of loads converges for a user defined "stagger" time step as shown in figure 3.

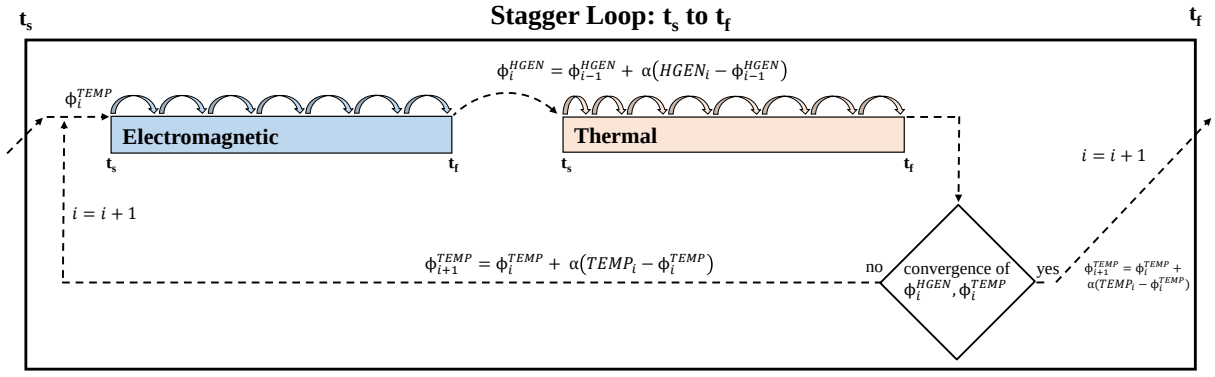

Figure 3: A stagger loop within the Multi-field Solver is shown for coupled electromagnetic and thermal fields (see figure 4 for an example of how such a simulation is set up with the user elements). In this example, the loads transferred between fields are heat generation ϕ^{HGEN} and temperature ϕ^{TEMP}. This approach loops over the stagger time step (from t_s to t_f) with a relaxation factor α applied to the load transfer until convergence of the loads is achieved. Separation of the problem into sequentially defined stagger steps is used to simulate over the entire time domain.

This solver has been successfully used for fully coupled simulations including the user elements. To do this, two physics fields are created which are shown labeled as "electromagnetic" and "thermal" in Figure 4. A load transfer interface is specified between meshed coil regions and any structural regions with eddy currents. This allows for passing Joule heat loads from the electromagnetic region to the thermal region, and passing temperature back. Both temperature and Joule heating are standard loads which may be transferred with the Multi-field Solver. To allow for thermal material properties to also vary with magnetic field and quench state, these variables are shared at every FEM iteration.

The method used for passing non-standard variables requires mesh element mapping be manually defined for user element regions. This is accomplished by using a similar mesh for matched regions between thermal and electromagnetic domains (AGEN is a useful command for this). Once a similar mesh has been created, the mapping is defined by setting real constant 1 of each thermal element as the matched element's number in the electromagnetic region. An example of a simple APDL script performing this mesh generation and matching is given in appendix B. With the element numbers manually mapped, the transfer of non-

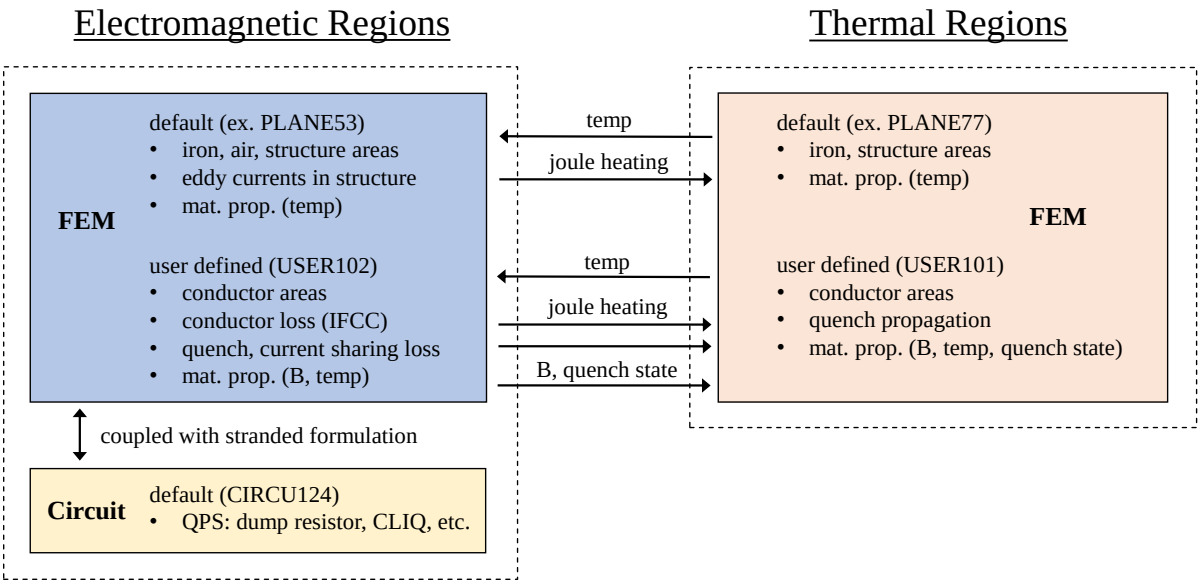

Figure 4: An overview of coupled thermal, electromagnetic, and circuit simulation in ANSYS with user defined elements is shown. Such an approach allows for simulating the impact of interfilament coupling currents, quench, and structural eddy currents on magnet behavior while including temperature and field dependent material properties. The independently meshed electromagnetic and thermal domains are solved concurrently using the Multi-field Solver.

standard MFS variables is performed during each element matrix generation.

7 Element Output

Table 4 lists the nodal and element results output to the ANSYS .db file. Nodal results are extrapolated from the four integration points to the corner nodes.

Table 4: USER102 Nodal and Element Output

Variable	Comp.	NSOL	ESOL	Description
AZ		yes	no	vector potential DOF
EMF		yes	no	voltage drop DOF
B	x	yes	yes	magnetic flux dens. comp.
B	y	yes	yes	magnetic flux dens. comp.
B	sum	yes	yes	magnetic flux dens. mag.
H	x	yes	yes	magnetic field intensity comp.
H	y	yes	yes	magnetic field intensity comp.
H	sum	yes	yes	magnetic field intensity mag.
JHEAT		no	yes	total element heat generation
VOLU		no	yes	element area

In addition to the standard results, a number of parameters are output as non-summable misc element results as described in Table 5. These can be plotted using "PLESOL,NMISC,#", where "#" is the corresponding number in the table.

Table 5: USER102 NMISC Output

NMISC	Variable	Description
(1)	T	elem temp used for mat. prop. etc.
(2)	B	elem field used for mat. prop. etc.
(3)	I0	elem current per turn
(4)	Jcw	elem current density in superconductor
(5)	Jc	critical current density for elem based on T,B
(6)	qflag	(-1) = SC, (0) = current sharing, (1) = quenched
(7)	Lc	effective length for coil resistance
(8)	Li	effective length for coil inductance
(9)	IFCU-mult	scale factor for IFCU
(10)	τ	IFCC time constant
(11)	JHres	resistive Joule heating
(12)	JHtau	IFCC Joule heating
(13)	JHeat	total Joule heating
(14)	IFCU	fraction of current in stabilizer for current sharing
(15)	RRR	copper RRR
(16)	fsc	SC fraction of conductor
(17)	fcond	conductor fraction of modeled coil area
(18)	rsvx	copper resistivity for elem based on T,B
(19)	elem	elem number
(20)	elflux	elem linked flux (nturns, length not included)
(21)	Mx	x comp. of IFCC magnetization
(22)	My	y comp. of IFCC magnetization
(23)		
(24)	rsvx/(fcond*(1-fsc))	scaled resistivity
(25)	J_{c0}	Nb_3Sn Jc fit parameter (in Equation 2)
(26)	T_{c0}	Nb_3Sn Jc fit parameter (in Equation 2)
(27)	B_{c0}	Nb_3Sn Jc fit parameter (in Equation 2)
(28)	α	Nb_3Sn Jc fit parameter (in Equation 2)
(29)	p	Nb_3Sn Jc fit parameter (in Equation 2)
(30)	τ-mult	scale factor for τ

8 Derivation of the Finite Element Matrices

8.1 A_z only

The finite element matrices (for the case of no circuit coupling) are derived from Maxwell's equations using a vector potential degree of freedom. This begins as

$$\nabla \times \frac{1}{\mu} \nabla \times \vec{A} = \vec{J}, \tag{19}$$

where the total current density $\vec{J}$ is the sum of an applied (source) current density $\vec{J}_s$ and a bound current density $\vec{J}_m$ which results from IFCC magnetization. The bound current can be re-written in terms of the degree of freedom as (see Eqn. 15)

$$\vec{J_m} = \nabla \times \vec{M}_e = \nabla \times \frac{-2\tau}{\mu_0} \frac{\partial}{\partial t} \left(\nabla \times \vec{A} \right). \tag{20}$$

The inclusion of $\vec{J_m}$ in Eqn. 19 and the consideration of $\mu = \mu_0$ in the conductor region leads to

$$\frac{1}{\mu_0} \nabla \times \nabla \times \vec{A} + \frac{2\tau}{\mu_0} \nabla \times \nabla \times \frac{\partial \vec{A}}{\partial t} = \vec{J}_s. \tag{21}$$

Here we see the treatment of IFCC as an equivalent magnetization leads to a damping term of similar form (curl-curl) as the stiffness term. The weak integral is used to derive the FEM matrices, so that

$$\int_\Omega \vec{N}_i \cdot \left[\frac{1}{\mu_0} \nabla \times \nabla \times \vec{A} + \frac{2\tau}{\mu_0} \nabla \times \nabla \times \frac{\partial \vec{A}}{\partial t} \right] dV = \int_\Omega \vec{N}_i \cdot \vec{J}_s dV. \tag{22}$$

Integrating the general vector identity

$$\int_\Omega \left[\vec{C} \cdot (\nabla \times \vec{D}) \right] dV = \int_\Omega \left[(\nabla \times \vec{C}) \cdot \vec{D} - \nabla \cdot (\vec{C} \times \vec{D}) \right] dV \tag{23}$$

and applying the divergence theorem can be used to show the volume integral of $\vec{C} \cdot (\nabla \times \vec{D})$ can be written as

$$\int_\Omega \left[\vec{C} \cdot (\nabla \times \vec{D}) \right] dV = \int_\Omega \left[(\nabla \times \vec{C}) \cdot \vec{D} \right] dV - \int_{\partial\Omega} \left[(\vec{C} \times \vec{D}) \cdot \hat{n} \right] dS. \tag{24}$$

Considering the form of Equation 22, with $\nabla \times \vec{A}$ as $\vec{D}$, the weak form can be written as

$$\begin{aligned} &\int_\Omega \left[\frac{1}{\mu_0} (\nabla \times \vec{N}_i) \cdot (\nabla \times \vec{A}) \right] dV + \int_\Omega \left[\frac{2\tau}{\mu_0} (\nabla \times \vec{N}_i) \cdot (\nabla \times \frac{\partial \vec{A}}{\partial t}) \right] dV \\ &- \int_{\partial\Omega} \left[\left(\vec{N}_i \times (\nabla \times \vec{A}) \right) \cdot \hat{n} \right] dS - \int_{\partial\Omega} \left[\left(\vec{N}_i \times (\nabla \times \frac{\partial \vec{A}}{\partial t}) \right) \cdot \hat{n} \right] dS \\ &= \int_\Omega \vec{N}_i \cdot \vec{J}_s dV \end{aligned} \tag{25}$$

With element shape functions used for both the test and basis functions (Galerkin), the element matrices in

$$\left[C^{AA}\right]\frac{\partial}{\partial t}\left\{A\right\}+\left[K^{AA}\right]\left\{A\right\}=\left\{J^{S}\right\} \tag{26}$$

are given by

$$\boxed{\left[C^{AA}\right]=f_{cond}\frac{2\tau}{\mu_0}\int\left[\left(\nabla\times\left[N_A\right]^T\right)^T\left(\nabla\times\left[N_A\right]^T\right)\right]dV_{elem}} \tag{27}$$

$$\boxed{\left[K^{AA}\right]=\frac{1}{\mu_0}\int\left[\left(\nabla\times\left[N_A\right]^T\right)^T\left(\nabla\times\left[N_A\right]^T\right)\right]dV_{elem}} \tag{28}$$

$$\boxed{\left\{J^{S}\right\}=\int\left\{J_S\right\}\left[N_A\right]^T dV_{elem}} \tag{29}$$

where the vector potential is written in terms of shape functions and the values at the element nodes A_e as

$$\left\{A\right\}=\left[N_A\right]^T\left\{A_e\right\} \tag{30}$$

with N_A being a matrix of the element shape functions.

As a check, equations 28 and 29 match the stiffness matrix and load vector in the ANSYS theory manual for PLANE53 [9]. The new damping matrix resulting from the equivalent magnetization also clearly matches the form of the stiffness matrix as expected. Note that for the damping matrix, the magnetization is scaled by the factor f_{cond} which is the ratio of conductor to the total modeled coil area (entered as a real constant). The building of these matrices is programmed in the user element Fortran files using Gaussian integration with the shape functions and integration points also programmed by the user.

8.2 A_z, $e(t)$, $i(t)$

The coupling to an external circuit follows the method developed for the standard distribution PLANE53 element [10], with several modifications to account for quench effects and separate effective lengths for coil resistance and inductance. A stranded formulation is used which adds a current $i(t)$ and emf $e(t)$ degree of freedom (DOF) to the vector potential given in Equation 26. Both these new DOF are constrained to be single values for a modeled coil region, with $i(t)$ being the current per stranded coil turn, and $e(t)$ being the voltage drop across the coil. The voltage drop is made up of both a resistive V_R and inductive V_L contribution such that

$$e(t)=V_R+V_L. \tag{31}$$

8.2.1 Resistive Voltage

The resistive voltage drop for a general stranded coil is given by

$$V_R = i(t)\sum_{i=1}^{N_c} R_i = i(t)\sum_{i=1}^{N_c}\frac{L_c}{\int \sigma dA_i} = i(t)\sum_{i=1}^{N_c}\frac{L_c N_c}{\int \sigma dS} = i(t)\frac{L_c N_c^2}{\int \sigma dS}. \tag{32}$$

where N_c is the number of coil turns, $i(t)$ is the current per turn, and L_c is an effective length chosen to best match the resistance of the 3D coil. It is convenient to reformat this into a volume integral such that

$$V_R = i(t)\frac{L_c N_c^2}{\int \sigma dS}\left(\frac{\int \rho dS}{\int \rho dS}\right)\frac{dv}{L_c dS} = i(t)\left(\frac{N_c}{S_c}\right)^2 \int \rho dV. \tag{33}$$

This is further adjusted to account for quench and current sharing effects. Depending on quench state, the current is assumed to be in the superconductor only, split between the superconductor and stabilizer, or entirely in the stabilizer. In addition, the resistive voltage from the modeled region is assumed to be generated only by current flowing in the stabilizer. To account for this two modifications are made to Equation 33. The first is a factor to account for the fractional area of the copper with respect to the full modeled area, and the second is a scaling of the current to the fraction which is found in the stabilizer region (defined as I_{fcu}). With these adjustments, the resistive voltage drop is given by

$$V_R = i(t)\left(\frac{N_c}{S_c}\right)^2 \frac{I_{fcu}}{f_{cond}(1-f_{sc})}\int \rho_{st} dV, \tag{34}$$

or for a 2D element with effective resistive length L_c as

$$V_R = i(t)L_c\left(\frac{N_c}{S_c}\right)^2 \frac{I_{fcu}}{f_{cond}(1-f_{sc})}\int \rho_{st} dS. \tag{35}$$

8.2.2 Inductive Voltage

The inductive voltage is given by the time derivative of the linked flux

$$V_L = \frac{\partial \Phi}{\partial t} = N_c \frac{\partial}{\partial t}\int (\hat{t}\cdot\vec{A}) ds. \tag{36}$$

For a 2D model with current restricted to flow only in the z direction,

$$V_L = N_c \frac{\partial}{\partial t} L_i (t A_z), \tag{37}$$

where t is positive or negative one based on current direction and L_i is the effective length scaling of the inductance chosen to match the 3D magnet. Reformatted as a volume integral, this becomes

$$V_L = t\frac{N_c}{S_c}\int \frac{\partial Az}{\partial t} dV, \tag{38}$$

or for a 2D element

$$V_L = t\frac{N_c}{S_c} L_i \int \frac{\partial Az}{\partial t} dS. \tag{39}$$

8.2.3 Circuit Coupling

Circuit coupling is accomplished by the addition of Equation 31 to the original vector potential formulation in Equation 26. In matrix form this is

$$\begin{aligned}\left[C^{AA}\right]\frac{\partial}{\partial t}\{A\}+\left[K^{AA}\right]\{A\}+\left[K^{Ai}\right]\{i(t)\}&=\{0\}\\ \left[C^{eA}\right]\frac{\partial}{\partial t}\{A\}+\left[K^{ee}\right]\{e(t)\}+\left[K^{ei}\right]\{i(t)\}&=\{0\}.\end{aligned}\tag{40}$$

With respect to PLANE53, a new matrix C^{AA} is included for the interfilament coupling currents, and the voltage balance matrices K^{ei} and C^{eA} are modified to include the changes mentioned for Equations 35 and 39. To enforce a single value for the voltage drop and current for each modeled coil region, the $i(t)$ and $e(t)$ DOF of the nodes in each coil region are coupled.

8.2.4 Element Matrices in 2D

The C^{AA} and K^{AA} matrices in 2D are found by simply reducing the general form already given in Equations 27 and 28. For the stranded conductor, the source term is now supplied by the circuit and determines the form of K^{Ai}. Considering the weak integral of the source term in 2D ($\vec{J}$ is now a scalar Jz), and that the current density of the stranded conductor is derived from the current per turn $i(t)$ using $J_z=\frac{N_c}{S_c}ti(t)$ leads to

$$\int\{N\}J_z dS=\int\{N\}\frac{N_c}{S_c}t\{N\}^T\{i(t)\}dS.\tag{41}$$

Here clearly the K^{Ai} matrix is given by

$$\boxed{\left[K^{Ai}\right]=-\frac{tN_c}{S_c}\int\{N\}\{N\}^T dS_{elem}.}\tag{42}$$

The 2D matrices in the voltage balance are derived from Equations 31, 35, and 39. The $e(t)$ term is re-written as an area integral with the shape functions added, such that

$$\begin{aligned}&t\frac{N_c}{S_c}L_i\int\{N\}^T\frac{\partial}{\partial t}\{Az\}dS-\frac{1}{S_c}\int\{N\}^T\{e(t)\}dS\\ &+L_c\left(\frac{N_c}{S_c}\right)^2\frac{I_{fcu}}{f_{cond}(1-f_{sc})}\rho_{st}\int\{N\}^T\{i(t)\}dS=0.\end{aligned}\tag{43}$$

Ansys solves the three DOF using the following form

$$\begin{bmatrix}C^{AA}&0&0\\C^{eA}&0&0\\0&0&0\end{bmatrix}\begin{bmatrix}\frac{\partial A}{\partial t}\\0\\0\end{bmatrix}+\begin{bmatrix}K^{AA}&0&K^{Ai}\\0&K^{ee}&K^{ei}\\0&0&0\end{bmatrix}\begin{bmatrix}A\\e\\i\end{bmatrix}=\begin{bmatrix}0\\0\\0\end{bmatrix}.\tag{44}$$

To match the sizing of the submatrices here, the vectors in Equation 43 are expanded to square matrices using the outer product with an identity vector $\{I\}$. This leads to 2D element matrices of

$$\boxed{\left[C^{eA}\right] = t\frac{N_c}{S_c}L_i \int \{I\}\{N\}^T dS_{elem}} \tag{45}$$

$$\boxed{[K^{ee}] = -\frac{1}{S_c}\int \{I\}\{N\}^T dS_{elem}} \tag{46}$$

$$\boxed{\left[K^{ei}\right] = L_c\left(\frac{N_c}{S_c}\right)^2 \frac{I_{fcu}}{f_{cond}(1-f_{sc})}\rho_{st}\int \{I\}\{N\}^T dS_{elem}} \tag{47}$$

The user element is coupled to an external circuit as voltage source using the standard distribution, circuit element CIRCU124. With key option one set to select a stranded coil, this element consists of three nodes labeled i, j, and k. The first two nodes are connected to adjacent circuit elements and each carry a single voltage DOF. The third node carries both a current and voltage drop DOF, and is chosen as one of the nodes in the meshed coil region to make it part of the coupled set. The stiffness matrix for the stranded coil CIRCU124 element is given by

$$\begin{bmatrix} 0 & 0 & 1 & 0 \\ 0 & 0 & -1 & 0 \\ -1 & 1 & 0 & s \\ 0 & 0 & 0 & 0 \end{bmatrix} \begin{bmatrix} V_i \\ V_j \\ i_k \\ e_k \end{bmatrix} = \begin{bmatrix} 0 \\ 0 \\ 0 \\ 0 \end{bmatrix}, \tag{48}$$

where s is a factor to account for modeling of a symmetric region. This couples the stranded coil into an external circuit which may be made up of additional coil regions or generic circuit elements selected using other key options for CIRCU124.

9 Benchmarking and Verification

Two verification and benchmarking studies have been performed. The first compares results for a single strand in a uniformly changing background field to analytic expectations. This study can be found in [11]. The second effort compares results from ANSYS to a similar implementation in COMSOL [12, 13] with the help of CERN. This extensive comparison can be found documented in [14].

A Known Limitations and Issues

Many of these are somewhat "easy" to implement or fix, but have been skipped over to get something up and running. There are also very few warnings set up for ill-defined input (mismatching keyopts, real constants, etc.) and unfortunately most problems will lead to a crash of ANSYS with no further output for debugging.

- General
  - the axisymmetric option is not yet included (contact lnbrouwer@lbl.gov if desired)
  - the Bi-2212 option is not yet included (contact lnbrouwer@lbl.gov if desired)
  - degenerate elements have issues (force quad mesh for user elem regions)
  - only compiled for single processor (run using SMP with 1 core)
  - no effort put into programming optimization for run time
  - no warnings if material property functions called beyond defined temperature range
- For Multi-field Solver (see Section 6 for more details)
  - marked load transfer regions must have similar mesh
  - thermal elements must be flagged for load transfer using real const
- USER101
  - recommended use is for conductor regions only (use PLANE77 elsewhere)
  - loading outside of HGEN (on lines etc.) may have issues
- USER102
  - recommended use is for conductor regions only (use PLANE53 elsewhere)
  - Lorentz forces are not yet included in the output

B Example: Element Mapping for MFS

This APDL script demonstrates how to generate and manually map a thermal domain from a previously created electromagnetic domain for the Multi-field Solver (see Section 6). Prior to this script, a group of several areas named "cond" has been created and meshed with USER102 (electromagnetic) elements. This scripts generates a new meshed area for each area in "cond", and sets real constant 1 of the new mesh elements to match the corresponding element number in the original electromagnetic region. The new regions are then grouped under the name "tcond" and the new mesh is modified to the thermal user element USER101.

```
!*************************************************************************
!****** Strand Element Mapping from Magnetic to Thermal  *******
!*************************************************************************

!match elements with a constant shift instead (no loop - much faster)
alls
numcmp,elem

cmsel,s,cond
alls,below,area
*get,nna,area,,count
*do,j,1,nna
 *get,na%j%,area,0,nxth
 asel,u,area,,na%j%
*enddo

! starting number for the real constants -> make sure no overlap with previously defined real constants
cnt = 500     !this needs to be greater than all other reals
*do,j,1,nna
     asel,s,area,,na%j%
     alls,below,area
     *get,enum,elem,,count
     *get,eMi,elem,,num,min

     agen,2,all,,,,,,0
     asel,u,area,,na%j%
     cm,tcond%j%,area

     cmsel,s,tcond%j%
     alls,below,area
     *get,eTi,elem,,num,min


     *do,i,1,enum
          r,cnt,eMi+(i-1)
          ettt = eTi+(i-1)
          esel,s,elem,,ettt
          emodif,all,real,cnt
          cnt = cnt + 1
     *enddo

*enddo

cmsel,s,tcond1
*do,j,2,nna
     cmsel,a,tcond%j%
*enddo
alls,below,area
cm,tcond,area

!*************************************************
!****** Define EMAG/THERMAL Interfaces  ***********
!*************************************************

cmsel,s,cond
cmsel,a,tcond
alls,below,area
bfe,all,fvin,,1      !define interfaces on both elements

!*************************************************
!****** Change Thermal Region Mesh to USER101 *****
!*************************************************

! thermal for conductor region only
et,12,user101
keyopt,12,1,0          ! 0=internal fits, 1=ANSYS table
keyopt,12,2,1          ! 0=no transfer to mag, 1=transfer to mag

cmsel,s,tcond
alls,below,area
emodif,all,mat,11
emodif,all,type,12
```

References

[1] "ANSYS Mechanical APDL Theory Reference, Release 12.0," 2009.

[2] K. J. Bathe, *Finite Element Procedures in Engineering Analysis*. Prentice-Hall, 1982.

[3] G. Manfreda, "Review of ROXIE's Material Properties Database for Quench Simulation," *CERN Internal Note: EDMS NR*, vol. 1178007, 2018.

[4] S. Russenschuck, *Field Computation for Accelerator Magnets: Analytical and Numerical Methods for Electromagnetic Design and Optimization*. Wiley-VCH, 2010.

[5] Z. J. J. Stekly and J. L. Zar, "Stable Superconducting Coils," *IEEE Transactions on Nuclear Science*, vol. 12, no. 3, p. 367, 1965.

[6] G. Morgan, "Theoretical Behavior of Twisted Multicore Superconducting Wire in a Time-Varying Uniform Magnetic Field," *Journal of Applied Physics*, vol. 41, p. 3673, 1970.

[7] M. Wilson, *Superconducting Magnets*. Oxford University Press, 1983.

[8] "ANSYS Mechanical APDL Coupled-Field Analysis Guide, Release 17.1," 2016.

[9] "ANSYS Mechanical APDL Theory Reference, Release 17.1," 2016.

[10] J. Wang, "A nodal analysis approach for 2d and 3d magnetic-circuit-coupled problems," *IEEE Trans. Magn.*, vol. 32, no. 4, pp. 1074–1077, 1996.

[11] L. Brouwer, "Check of IFCC Equivalent Magnetization Implementation in ANSYS User Elements using a Single Strand Model," *LBNL Eng. Note: SU-1010-4842, R1.0*, 2019. [Online]. Available: https://usmdp.lbl.gov/scpack-code/

[12] L. Bortot, B. Auchmann, I. Cortez-Garcia, A. M. Fernandez-Navarro, M. Maciejewski, M. Mentink, M. Prioli, E. Ravaioli, S. Schops, and A. Verweij, "Steam: A hierarchical co-simulation framework for superconducting accelerator magnet circuits," *IEEE Trans. Appl. Supercond.*, vol. 28, no. 3, p. 4900706, 2018.

[13] L. Bortot, B. Auchmann, I. Cortez-Garcia, A. M. Fernandez-Navarro, M. Maciejewski, M. Prioli, S. Schops, and A. Verweij, "A 2-d finite-element model for electro-thermal transients in accelerator magnets," *IEEE Trans. Appl. Supercond.*, vol. 54, no. 3, p. 7000404, 2018.

[14] L. Brouwer, B. Auchmann, L. Bortot, and E. Stubberud, "Crosscheck of the ANSYS-COMSOL 2D FEM Implementations for Superconducting Accelerator Magnets," *LBNL Eng. Note: SU-1010-4841, R1.0*, 2019. [Online]. Available: https://usmdp.lbl.gov/scpack-code/